American Mineralogist, Volume 88, pages 1324–1330, 2003

The atomic arrangement of the ganophyllite-group modulated layer silicates as determined from the orthorhombic dimorph of tamaite, with the elusive 16.8 Å ganophyllite-group superstructure revealed

JOHN M. HUGHES,[1,*] JOHN RAKOVAN,[1] ROBERTO BRACCO,[2] AND MICKEY E. GUNTER[3]

[1]Department of Geology, Miami University, Oxford, Ohio 45056, U.S.A.
[2]Ferrania Imaging Technologies, 17014 Ferrania (SV), Italy
[3]Department of Geology, University of Idaho, Moscow, Idaho 83844-3022, U.S.A.

ABSTRACT

The ganophyllite-group minerals, with general formula (K, Na, Ca)$_x$Mn$_6$(Si$_9$Al)O$_{24}$(OH)$_4$·nH$_2$O (ganophyllite = K, eggletonite = Na, tamaite = Ca), are complex modulated layer silicates that contain 2:1 trioctahedral layers with Mn^{2+}-O$_6$ octahedra. Pervasive superstructures have frustrated the numerous attempts at solution of the atomic arrangement of these modulated layer silicates. An orthorhombic dimorph of tamaite has been discovered and its atomic arrangement solved, elucidating the elusive structure of the ganophyllite-group minerals. The dimorph was discovered in the Val Graveglia mining district in the northern Apennines, approximately 35 km east of Genoa, Italy. The phase crystallizes in space group *Pnma*, a = 16.8146(6), b = 25.2036(9), c = 13.3866(5) Å. The weak reflections from the 3× "superstructure" along **a**, long observed but never successfully measured in ganophyllite-group minerals, were obtained using a CCD detector and subsequently the atomic arrangement was solved and refined (R = 0.079). The structural modulation in ganophyllite-group minerals results from the misfit between the sheets of $Mn^{2+}O_6$ octahedra and silicate tetrahedra. The atomic arrangement consists of corrugated *T*-O-*T* layers, with inverted tetrahedra in the tetrahedral sheets connecting adjacent layers along **b**. The inverted tetrahedra exist as four-member rings, and incorporate Al, with a maximum Al occupancy of Si$_{2.00}$Al$_{2.00}$. Charge balance for the substituent Al is maintained by adding cations (Ca, K, Na) or $^{[6]}$Al sufficient to balance the charge lost by the Al ↔ Si substitution in the interlayer tetrahedra. Zeolitic H$_2$O molecules also exist in the interlayer channels. Contrary to earlier speculation, the 5.6 Å "subcell" (along **a** in the orthorhombic dimorph) observed in ganophyllite-group phases is not a true subcell, in that it does not have approximately equivalent atoms at (x, y, z), [~(x + 1/3), ~y, ~z], and [~(x + 2/3), ~y, ~z) for all atoms. Although the majority of the cation scattering (all Mn + 2/3 of the Si atoms) exist in a supercell-subcell relationship, as manifested in very strong $h = 3n$ and very weak (heretofore immeasurable) $h \neq 3n$ reflections, the lack of such a relationship for all atoms prohibited a successful solution based on previous assumptions of a subcell-supercell relationship.

INTRODUCTION

Ganophyllite, ideally (K,Na,Ca)$_6$(Mg,Fe,Mn)$_{24}$(Si$_{32.5}$Al$_{7.5}$)O$_{96}$(OH)$_{16}$·21H$_2$O, is a complex modulated layer silicate that contains 2:1 trioctahedral layers of Mn^{2+} dominant octahedra and silicate tetrahedra; the structural modulation arises from the misfit between the large manganese octahedra and the silicate tetrahedra in the *T*-O-*T* layers (Eggleton and Guggenheim 1986). Peacor et al. (1984) have described eggletonite, the Na-dominant end-member of ganophyllite, and tamaite, described by Matsubara et al. (2000), is the calcium-dominant end-member of the ganophyllite-group.

The atomic arrangement of the ganophyllite-group minerals has been extensively studied but the structure solution has remained elusive, perhaps due to the atomic perturbations that cause the pervasive superstructures. Noe and Veblen (1999) recently recounted the attempts at unraveling the atomic arrangement of ganophyllite and reported a refinement of the ganophyllite subcell and a proposed model of the supercell. We refer the reader to that study for an excellent detailed summary of previous work and conjecture on the atomic arrangement of ganophyllite-group phases.

One of the authors (R.B.) recently collected specimens of a Ca-dominant member of the ganophyllite group from the Val Graveglia mining district in the northern Apennines, approximately 35 km east of Genoa, Italy. Examination of our Ca-dominant phase showed, unlike monoclinic ganophyllite, eggletonite, and tamaite, that the Val Graveglia material was orthorhombic, and thus is the orthorhombic dimorph of tamaite. A review of the literature revealed that the natural Ca-dominant orthorhombic phase had also been recognized by Mottana et al. (1990) but was not described as a new mineral. The orthorhombic material was suitable for structure analysis, and a CCD-based diffractometer allowed measurement of the pervasive

* E-mail: hughesjm@muohio.edu

weak reflections that result from superstructures in the compound; these weak reflections have prevented previous structure solutions. We successfully solved the crystal structure of the orthorhombic dimorph of tamaite, for the first time elucidating the atomic arrangement and the 3×5.6 Å superstructure observed in ganophyllite-group minerals. We present here the atomic arrangement of the orthorhombic dimorph of tamaite that illustrates the elusive atomic arrangement of the ganophyllite-group minerals. To clarify the structural relations among the ganophyllite-group minerals, Table 1 presents the unit-cell parameters for the four member phases.

GEOLOGICAL SETTING AND OCCURRENCE

Ganophyllite-group minerals are known from several metamorphic manganese deposits, including the Kombat mine (Namibia), Franklin (New Jersey), and the type locality, Långban (Sweden), but Val Graveglia, Italy is likely the most productive locality for these minerals. The Val Graveglia mining district is located in the northern Apennines, approximately 35 km east of Genoa, and has been exploited for over a century in several sites of which only Gambatesa (for which the area is also known) is active today.

Val Graveglia is probably unique among manganese fields in its genetic and metamorphic history. The primary ocean-bottom deposition of sediments was followed by gravitative concentration and subsequent weak metamorphism (greenschist facies) during the Alpine uplift. The orogenic event further concentrated the mineralization, giving rise to the main ore bodies as thick braunite lenses. Another result of the Alpine orogenic event was the creation of a system of folds and fractures through which hydrothermal fluids altered the primary ore into a suite of silicates and carbonates (Marescotti and Frezzotti 2000). Later circulation in post-orogenic recovery fractures mobilized rare elements, resulting in a final generation of open-fissure mineralization. The over 100 mineral species known in Val Graveglia, eight of which are type-species, are thoroughly described in a recent paper (Marchesini and Pagano 2001), and the list is constantly updated by new finds. Manganese phyllosilicates, including bemenite, parsettensite, and ganophyllite, are widespread in the deposit.

The occurrence of euhedral crystals of ganophyllite-group phases is quite uncommon, and the specimens that are the subject of this study come from a unique find in 1986 at the now-closed Molinello mine. In that mine, the purported ganophyllite was found as equant, prismatic, translucent olive-green crystals associated with rhodonite in a veinlet cutting a phyllosilicate vein (Fig. 1).

TABLE 1. Unit-cell relations among ganophyllite-group minerals

Mineral	Space group	*a*	*b*	*c* (Å)	β (°)
This work*	*Pnma*	16.8146(6)	25.2036(9)	13.3866(5)	90
Tamaite†	$P2_1/a$	16.64(1)	27.11(2)	25.35(2)	98.74(7)
Eggletonite‡	*/2/a* or */a*	5.554	13.72	25.00	93.95
Ganophyllite§	*A*2/*a*	16.60(5)	27.04(8)	50.34(15)	94.17(17)

* For direct comparison with other phases in Table 1, *b* and *c* axes of orthorhombic phase should be reversed to yield $a\bar{c}b$ *Pnam* setting of *Pnma*.
† Matsubara et al. (2000).
‡ Peacor et al. (1984).
§ Smith and Frondel (1968).

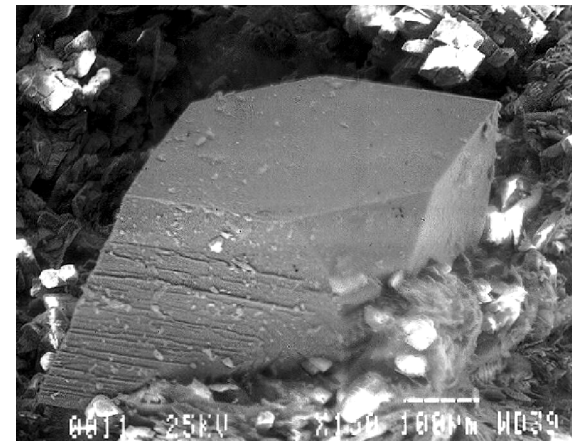

FIGURE 1. SEM image of a crystal from the Molinello Mine, Val Graveglia, Italy (image courtesy of S. Magnanelli, Ferrania Imaging Technologies). Scale bar 100 µm.

PHYSICAL AND OPTICAL PROPERTIES

Because of the similarity of the orthorhombic dimorph of tamaite to other ganophyllite group phases, many of their physical properties are similar, and without chemical analyses it is difficult if not impossible to distinguish between them.

The sample used in this study is honey-yellow, translucent to transparent, with a vitreous luster and a white streak. The mineral has a Mohs hardness of 4–4.5, is brittle, and displays excellent {010} cleavage. It has a calculated density of 2.67 g/cm^3, and a measured density, by sink-float methods, of 2.77 g/cm^3.

The optical properties were measured using 589.3 nm wavelength light; the mineral is biaxial (–), with $\alpha = 1.5546(5)$, $\beta = 1.5985(5)$, $\gamma = 1.5995(5)$, and $a = Z$. Pleochroism was observed as X = light brown, Y = light blue-green, and Z = green. The calculated value of $2V_x$ is 17°, and the observed valued is 10°. The compatibility index is 0.003, which is in the excellent range (Mandarino 1981).

EXPERIMENTAL METHODS

Crystal structure

A crystal of purported ganophyllite was separated from the samples from Val Graveglia. Intensity data were collected on a Bruker Platform goniometer equipped with an APEX 4K CCD detector and Mo$K\alpha$ radiation; reflections of the ($3 \times$ ~5.6 Å) superstructure were recognized by the standard cell-searching routines. Data were integrated using the Bruker program SAINT, and absorption was corrected using the program SADABS. The structure was first solved in space group $P2_1/n$ using direct methods and Fourier synthesis as implemented in the Bruker program package SHELXTL version 6.10. Subsequent evaluation showed that the atomic arrangement was better described in the supersymmetric space group *Pnma*, and thus the data were re-integrated and refined in *Pnma*. This is consistent with the results of Mottana et al. (1990), who determined a = 16.782, b = 13.370, c = 25.090 Å and space group *Pnam* (a reorientation of *Pnma*) or $Pna2_1$, from single crystal X-ray diffraction data.

Least-squares refinement was undertaken using the Bruker program SHELXTL version 6.10, using neutral-atom scattering factors and corrections for anomalous dispersion. The refinements were routine, and all atomic thermal ellipsoids were positive-definite; hydrogen atoms associated with hydroxyl groups were located in difference maps and their positions were successfully refined. The thermal parameters for several atoms in the framework (O26, O27, O28) suggested that the atoms were disordered, but the disorder was not suc-

cessfully modeled; similar disorder was noted in the study of Noe and Veblen (1999). Additional positional disorder, as well as the existence of partially occupied sites, was noted in the "channel" occupants (H_2O, Na, K). Noe and Veblen (1999) noted that many of the interlayer sites were partially occupied, were split, or refined with unreasonable displacement parameters despite the fact that they went to great lengths to refine atomic positions using various structural constraints. They also noted that many additional partially occupied sites (presumably occupied by H_2O) existed, and were not modeled. We too found that the largest electron-density residuals [all peaks ≤2.53(8) $e^-/Å^3$] exist in that region. The subsequent structure discussion shows that occupants of the interlayer channels are weakly constrained, and are essentially zeolitic in nature. Many of the difficulties associated with the structure work of Noe and Veblen (1999) (such as the unreasonable Si-O distances, ranging from 1.27 to 2.09 Å) undoubtedly arose from the refinement in a subcell of the correct cell, a pitfall noted by those authors but alleviated by the CCD detector used in this study.

Table 2 contains crystal data and results of the structure refinement, and Table 3 contains atomic parameters. Table 4 gives selected interatomic distances and bond-valence sums for non-hydrogen cations. Tables 5 and 6[1] give anisotropic thermal parameters and calculated and observed structure factors for the orthorhombic dimorph of tamaite.

Chemical analysis

Subsequent to structure determination, samples of purported ganophyllite were prepared for electron microprobe analysis (EMPA). Data were collected with a Cameca SX-100 electron microprobe at the New Mexico Bureau of Mines and Mineral Resources, Soccoro, New Mexico. The microprobe was operated at 15 kV and 19.9 nA; mineral samples were used as standards. The concentrations of Ca, Na, and K were found to be heterogeneous. Fourteen spots were analyzed and the CaO values ranged from 1.11 to 1.33 wt%, the Na_2O concentrations from 0.16 to 0.69 wt%, and the K_2O contents from 0.12 to 2.04 wt%. In eleven of the fourteen analyses Ca was the dominant channel cation. Table 7 contains the average results of the 14 analyses and presents the empirical formula. The EMPA results showed that Ca was the dominant species in the alkali/alkaline earth sites in the structural channels, thus the dimorph of tamaite was recognized. Mottana et al. (1990) also determined that the material was compositionally heterogeneous; their analyses showed that the concentration of Ca was greater than K or Na in two of thirteen analyzed spots.

Two types of H_2O are recognized in the analyses, as elucidated subsequently in the details of the structure analysis. These include the structurally bound hydroxyl groups in the octahedral sheet, in addition to the loosely bound zeolitic water molecules in the channels. Total H_2O was determined by difference; after assignment of $(OH)_4$ as determined in the structure analysis, the remainder was assigned as zeolitic water.

As discussed below, (2Ca + K + Na) + $^{[6]}$Al = $^{[4]}$Al in ganophyllite-group minerals, as the channel alkalies/alkaline earth elements plus minor substituent $^{[6]}$Al must balance the charge lost from incorporation of $^{[4]}$Al in the interlayer tetrahedra. On the basis of the EMPA results and a formula basis of (Mn + Mg + Fe + Al + Si) = 16, (2Ca + K + Na) + $^{[6]}$Al = 1.00 (the exact maximum amount allowed because of limitations in $^{[4]}$Al incorporation), and $^{[4]}$Al = 0.85 (Table 7).

[1] For a copy of Tables 5 and 6, Document AM-03-038, contact the Business Office of the Mineralogical Society of America (see inside front cover of recent issue) for price information. Deposit items may also be available on the *American Mineralogist* web site at http://www.minsocam.org.

TABLE 2. Crystal data and parameters of structure refinement for orthorhombic dimorph of tamaite

Space group	*Pnma*
Unit-cell parameters (refined from 7,861 reflections)	
a (Å)	16.8146(6)
b (Å)	25.2036(9)
c (Å)	13.3866(5)
Frame width	0.20°
Scan time	10 s
Number of frames	3600
Detector distance	6.059 cm
Effective transmission	0.749341–1.000
R_{int} (–)	
before SADABS absorption correction	0.0667
after SADABS absorption correction	0.0321
Measured reflections, full sphere	67 408
Unique reflections	7121
Refined parameters	462
*R*1	0.0786 for 5795 unique data, $I > 4\sigma_I$ data
*R*1	0.0950 for 7121 unique
Largest difference peaks	+2.53(8), –2.16(8) $e^-·Å^{-3}$
Goodness-of-Fit	1.061

TABLE 3. Atomic positions and equivalent isotropic *U* for atoms in orthorhombic dimorph of tamaite

Atom	*x*	*y*	*z*	U_{eq}
Mn1	–0.58201(5)	–0.01781(4)	0.30893(7)	0.0135(2)
Mn2	–0.58477(5)	–0.99737(4)	0.55744(7)	0.0133(2)
Mn3	–0.74898(5)	–0.01450(4)	0.42999(7)	0.0151(2)
Mn4	–0.74917(6)	–0.00989(5)	0.17972(7)	0.0195(2)
Mn5	–0.91573(6)	–0.01802(4)	0.30845(7)	0.0169(2)
Mn6	–0.58239(5)	–0.00233(4)	0.05744(6)	0.0092(2)
Si1	–0.87449(9)	–0.11773(7)	0.4679(1)	0.0090(3)
Si2	–0.85372(9)	–0.11855(7)	0.1378(1)	0.0110(3)
Si3	–0.53570(9)	–0.12257(7)	0.1419(1)	0.0094(3)
Si4	–0.4746(2)	–0.90508(9)	0.3040(1)	0.0365(6)
Si5	–0.6939(1)	–0.10480(7)	0.0262(1)	0.0117(3)
Si6	–0.48436(9)	–0.88666(7)	0.5307(1)	0.0095(3)
Si7	–0.1349(2)	–0.90364(9)	0.3056(1)	0.0406(7)
Si8	–0.3071(2)	–0.90682(10)	0.2005(2)	0.0397(6)
Si9	–0.70962(9)	–0.81341(7)	0.8138(1)	0.0106(3)
Si10	–0.39833(9)	–0.81326(7)	0.6817(1)	0.0104(3)
O1H	–0.6393(3)	–0.9679(2)	0.4241(3)	0.0152(9)
H1	–0.639(5)	–0.938(4)	0.421(6)	0.02(2)
O2H	–0.6942(3)	–0.0422(2)	0.5670(3)	0.0145(9)
H2	–0.700(7)	–0.079(5)	0.582(9)	0.07(4)
O3H	–0.6961(3)	–0.0544(2)	0.3020(3)	0.0147(9)
H3	–0.698(9)	–0.089(6)	0.31(1)	0.10(5)
O4	–0.6344(3)	–0.9663(2)	0.1848(3)	0.021(1)
O5	–0.8074(3)	–0.9697(2)	0.3045(3)	0.020(1)
O6	–0.8617(3)	–0.0563(2)	0.4393(3)	0.0163(9)
O7	–0.8594(2)	–0.0569(2)	0.1703(3)	0.0143(9)
O8H	–0.4709(3)	–0.9664(2)	0.0710(3)	0.0169(9)
H8	–0.472(5)	–0.931(3)	0.086(6)	0.02(2)
O9	–0.5281(3)	–0.0623(2)	0.1814(3)	0.019(1)
O10	–0.4761(3)	–0.8772(2)	0.4114(3)	0.0188(9)
O11	–0.8697(3)	–0.1261(2)	0.5881(3)	0.0185(9)
O12	–0.4748(2)	–0.9487(2)	0.5548(3)	0.0117(8)
O13	–0.9622(2)	–0.1371(2)	0.4319(3)	0.0131(9)
O14	–0.0383(2)	–0.1663(2)	0.2714(3)	0.0171(9)
O15	–0.1928(3)	–0.0415(2)	0.4580(3)	0.0159(9)
O16	–0.8059(3)	–0.8791(2)	0.4093(3)	0.024(1)
O17	–0.8047(3)	–0.8231(2)	0.7838(3)	0.0170(9)
O18	–0.0271(3)	–0.0316(2)	–0.1904(3)	0.0181(9)
O19	–0.0836(3)	–0.1496(2)	0.0803(4)	0.019(1)
O20	–0.5720(3)	–0.8664(2)	0.5649(3)	0.0152(9)
O21	–0.7269(3)	–0.8702(2)	0.5741(3)	0.018(1)
O22	–0.6470(3)	–0.8416(2)	0.7317(3)	0.0176(9)
O23	–0.6156(2)	–0.1305(2)	0.0751(3)	0.018(1)
O24	–0.6827(4)	3/4	0.8214(5)	0.019(1)
O25	–0.0793(4)	1/4	0.1583(5)	0.019(1)
O26	–0.3916(8)	–0.8848(3)	0.2515(8)	0.125(6)
O27	–0.2215(8)	–0.8860(3)	0.2539(8)	0.112(5)
O28	–0.055(1)	–0.8849(3)	0.249(1)	0.165(8)
O29	–0.6929(3)	–0.8436(2)	–0.0759(3)	0.020(1)
Ca	–0.5572(5)	1/4	0.734(1)	0.149(9)
K	–0.443(2)	1/4	0.424(3)	0.11(2)
H_2O	–0.693(2)	–1/4	0.084(1)	0.15(1)
H_2O2	–0.3175(9)	1/4	0.3200(8)	0.046(6)
H_2O3	–0.3061(8)	–0.685(1)	0.430(1)	0.13(1)
H_2O4	–0.612(2)	1/4	0.571(2)	0.13(2)

RESULTS AND DISCUSSION

The *Pnma* atomic arrangement of the ganophyllite group minerals is described in terms of three components: the sheets, the interlayer tetrahedra, and the channel constituents, and fi-

TABLE 4. Selected interatomic distances in orthorhombic dimorph of tamaite

Layer Octahedra			
Mn1-O3H	2.132(5), *0.40*	Mn2-O1H	2.140(5), *0.39*
Mn1-O1H	2.210(5), *0.32*	Mn2-O2H	2.164(5), *0.36*
Mn1-O18	2.217(5), *0.32*	Mn2-O18	2.203(5), *0.33*
Mn1-O12	2.226(4), *0.31*	Mn2-O12	2.218(4), *0.31*
Mn1-O9	2.234(5), *0.30*	Mn2-O7	2.244(4), *0.29*
Mn1-O4	2.286(5), *0.26*	Mn2-O12	2.260(4), *0.28*
Mean, Sum	2.218, *1.91*	Mean, Sum	2.205, *1.96*
Mn3-O2H	2.168(4), *0.36*	Mn4-O3H	2.175(5), *0.35*
Mn3-O6	2.172(5), *0.36*	Mn4-O5	2.185(5), *0.34*
Mn3-O3H	2.177 (4), *0.35*	Mn4-O7	2.203(4), *0.33*
Mn3-O1H	2.188(5), *0.34*	Mn4-O2H	2.216(5), *0.32*
Mn3-O5	2.250(5), *0.29*	Mn4-O15	2.221(4), *0.31*
Mn3-O15	2.279(4), *0.27*	Mn4-O4	2.221(5), *0.31*
Mean, Sum	2.206, *1.97*	Mean, Sum	2.204, *1.96*
Mn5-O5	2.192(5), *0.34*	Mn6-O8H	2.091(5), *0.44*
Mn5-O6	2.195(5), *0.33*	Mn6-O8H	2.093(5), *0.44*
Mn5-O9	2.198(5), *0.33*	Mn6-O15	2.112(5), *0.42*
Mn5-O18	2.234(5), *0.30*	Mn6-O4	2.120(5), *0.41*
Mn5-O8H	2.271(5), *0.27*	Mn6-O6	2.359(5), *0.21*
Mn5-O7	2.297(4), *0.25*	Mn6-O9	2.423(5), *0.18*
Mean	2.231, *1.82*	Mean	2.200, *2.10*
Layer Tetrahedra			
Si1-O29	1.605(5), *1.05*	Si2-O22	1.610(5), *1.04*
Si1-O6	1.610(5), *1.04*	Si2-O7	1.617(5), *1.02*
Si1-O11	1.626(5), *1.00*	Si2-O21	1.626(5), *0.99*
Si1-O13	1.627(4), *0.99*	Si2-O20	1.630(5), *0.98*
Mean, Sum	1.617, *4.08*	Mean, Sum	1.621, *4.03*
Si3-O14	1.601(5), *1.06*	Si3-O18	1.597(5), *1.08*
Si3-O9	1.614(5), *1.03*	Si3-O10	1.601(5), *1.07*
Si3-O13	1.623(4), *1.00*	Si3-O28	1.61(1), *1.04*
Si3-O23	1.626(4), *1.00*	Si3-O26	1.645(9), *0.95*
Mean, Sum	1.616, *4.09*	Mean, Sum	1.613, *4.14*
Si5-O21	1.607(5), *1.05*	Si6-O19	1.606(5), *1.05*
Si5-O23	1.607(5), *1.05*	Si6-O12	1.607(5), *1.05*
Si5-O15	1.610(5), *1.04*	Si6-O10	1.620(5), *1.01*
Si5-O16	1.617(5), *1.02*	Si6-O20	1.625(5), *1.00*
Mean, Sum	1.610, *4.16*	Mean, Sum	1.615, *4.11*
Si7-O4	1.585(6), *1.11*	Si8-O5	1.586(6), *1.11*
Si7-O11	1.610(5), *1.04*	Si8-O16	1.628(5), *0.99*
Si7-O28	1.61(1), *1.03*	Si8-O26	1.67(1), *0.88*
Si7-O20	1.67(1), *0.87*	Si8-O27	1.69(1), *0.84*
Mean, Sum	1.619, *4.05*	Mean, Sum	1.644, *3.82*
Interlayer Tetrahedra			
Si9-O24	1.664(3), *0.90*	Si10-O17	1.659(5), *0.91*
Si9-O17	1.667(5), *0.89*	Si10-O25	1.668(3), *0.89*
Si9-O22	1.679(5), *0.86*	Si10-O19	1.677(5), *0.87*
Si9-O29	1.685(5), *0.85*	Si10-O14	1.686(5), *0.84*
Mean, Sum	1.674, *3.50*	Mean, Sum	1.673, *3.51*
Interlayer Cations			
Ca*-H_2O4	2.36(4), *0.34*	K†- H_2O2	2.53(4), *0.34*
Ca*-O24	2.42(1), *0.30*	K†- H_2O3	2.83(4), *0.15*
Ca*-O25	2.51(1), *0.23*	K†- H_2O3	2.83, *0.15*
Ca*-O14	2.699(9), *0.14*	K†- O25	3.16(4), *0.06*
Ca*-O14	2.699, *0.14*	K†- O10	3.258(8), *0.05*
Ca*-O22	2.758(7), *0.12*	K†- O10	3.258, *0.05*
Ca*-O22	2.758, *0.12*	K†- O19	3.31(2), *0.04*
Mean, Sum	2.601, *1.39*	K†- O19	3.31, *0.04*
		Mean, Sum	3.061, *0.88*

Notes: Numbers in italics are bond valences of individual bonds and bond valence sums for polyhedra. Bond valences for Si1-Si8 tetrahedra were calculated using constants for Si. Bond valence constants from Brese and O'Keeffe (1991), except for universal constants for Al, Si in interlayer tetrahedra (Si9, Si10) (Brown 1981).

* Site occupied by $(Ca_{0.50}Na_{0.24}\square_{0.26})$; bond-valence values calculated using Ca constants.

† Site occupied by $(K_{0.34}\square_{0.66})$; bond-valence calculated using K constants.

TABLE 7. Chemical analytical data for the orthorhombic dimorph of tamaite (wt%)

Oxide	Mean	Range
SiO_2	48.12	46.45–50.29
TiO_2	0.03	0.00–0.05
Al_2O_3	4.70	4.49–4.88
Cr2O3	0.01	0.00–0.03
MnO	35.59	34.95–36.43
MgO	0.18	0.07–0.27
FeO	0.08	0.03–0.17
CaO	1.22	1.11–1.33
Na_2O	0.34	0.16–0.69
K_2O	0.71	0.08–2.04
F	0.01	0.00–0.12
H_2O*	9.01	7.27–10.95
Total	100.00	

Note: Empirical formula $[(Si + Al + Mn + Mg + Fe) = 16]$: $(Ca_{0.25}K_{0.17}Na_{0.12})(Mn_{5.73}Mg_{0.05}Fe_{0.01}Al_{0.21})(Si_{9.15}Al_{0.85})O_{24}(OH)_4 \cdot 3.72H_2O$.

* H_2O by difference from 100%; OH_4 assigned by structure analysis.

nally through the subcell-supercell relationship. The structure of the phase is illustrated in Figures 2 and 3.

The sheets in ganophyllite-group phases

As determined from the orthorhombic dimorph of tamaite, the sheets in ganophyllite-group phases are formed of infinite, two-dimensional sheets of $Mn^{2+}O_6$ octahedra that are sandwiched between sheets of SiO_4 tetrahedra, together forming modulated 2:1 layers. Table 4 lists the bond lengths of the octahedra, the layer tetrahedra, and the channel cations, and also bond-valences for the cation-O atom bonds.

Mn^{2+} is not a common octahedral sheet cation in layer silicates, and MnO_6 octahedra are larger than octahedra with more common occupants such as Al and Mg. The mismatch in size between the octahedral and tetrahedral components of the *T*-O-*T* layers creates a misfit between these two structural components. As depicted in Figure 2a, the misfit is manifested in an extreme corrugation of the 2:1 layer and modulation of the tetrahedra, which allows for registry between such mismatched sheets (Guggenheim and Eggleton 1997, 1998).

Figure 3 depicts a [010] projection of a tetrahedral sheet. As seen therein, the regular pseudohexagonal atom arrangement typical in layer silicates is interrupted by the bridging tetrahedra, which are inverted from those in the regular pseudohexagonal array. The silicate layer contains five-, six-, and seven-member tetrahedral rings, combining "normal" tetrahedra and inverted tetrahedra from the interlayer linkages. All tetrahedral bond lengths refined to reasonable values; bond-valence values demonstrate that only the inverted tetrahedra contain substituent Al (Table 4). During the refinement, three of the bridging O atoms (O26, O27, O28) were identified as possibly having positional disorder, as noted by Noe and Veblen (1999) for some of their tetrahedra. The split sites were not successfully refined, however.

The Mn atoms bond to O atoms and hydroxyl groups. Four of the O atoms bonding to the manganese atoms were identified as hydroxyl O atoms by examination of Pauling bond valences; none of the hydroxyl O atoms bond to Si atoms, as expected.

Interlayer tetrahedra

Inverted tetrahedra connect the layers in ganophyllite group minerals (Figs. 2a and 2b). The interlayer tetrahedra (Si9, Si10)

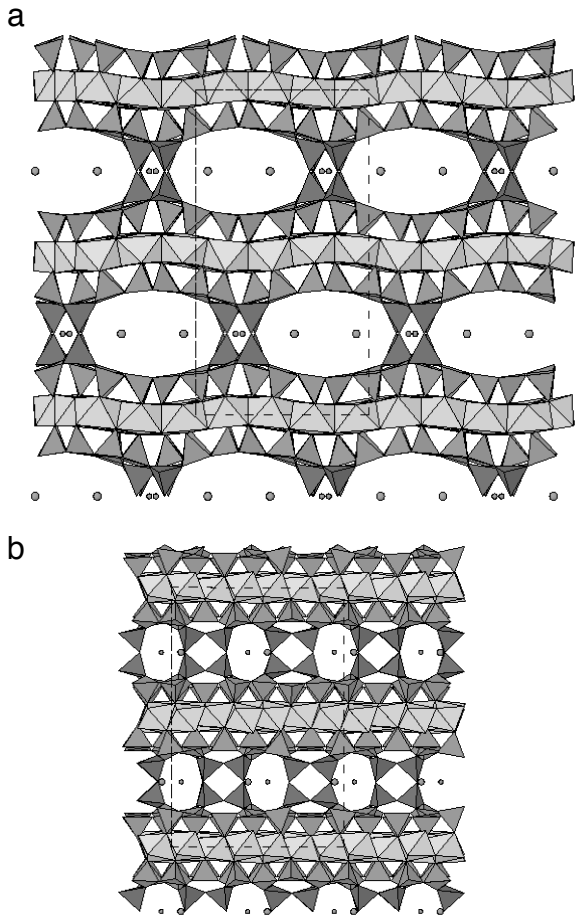

FIGURE 2. Atomic arrangement of the orthorhombic dimorph of tamaite. The unit cell is denoted by dashed line in both projections. Larger unbonded atoms are Ca, smaller are Na. H_2O molecules are not depicted. (**a**) Projection down [100]; **b** axis is vertical. (**b**) Projection down [001]; **b** axis is vertical. Atoms are the same as in **a**.

are incorporated in the silicate sheets, to which they bond through corner-sharing. The inverted tetrahedra link to other tetrahedra through all four vertices, and form four-member rings in the interlayer region (Fig. 2b).

The interlayer tetrahedra, in contrast to the non-inverted tetrahedra, incorporate Al. Table 4 lists the bond lengths for the tetrahedra, and illustrates that the interlayer tetrahedral bond lengths reflect incorporation of $^{[4]}$Al.

With no incorporation of substituent $^{[4]}$Al, the formula of the ganophyllite framework is neutral, and thus the incorporation of interlayer channel cations (Ca = tamaite and its orthorhombic dimorph; K = ganophyllite; Na = eggletonite) is not necessarily stoichiometric as previously assumed; the amount of substitution of interlayer cations reflects the equivalent amount of Al present in the interlayer tetrahedra. With no Al in the interlayer tetrahedra or the layer octahedra, the ganophyllite-group formula as derived from the crystal structure results is $Mn_6Si_{10}O_{24}(OH)_4{\cdot}nH_2O$, which is electrostatically neutral; the water molecules occupy the channel region. Thus

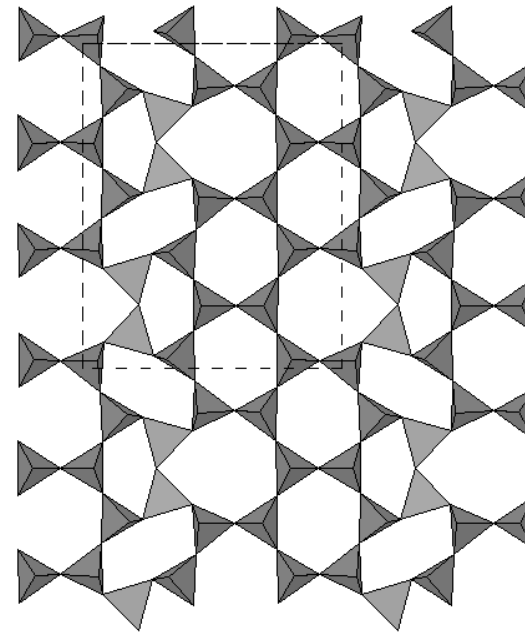

FIGURE 3. Structure of the orthorhombic dimorph of tamaite projected down [010]. The unit cell is denoted by the dashed line. The interlayer atoms are omitted, and the **a** axis is vertical. The light-colored tetrahedra link adjacent layers.

ganophyllite-group minerals contain interstitial cations (K, Na, $Ca_{0.5}$) only in proportion to the amount of $^{[4]}$Al in the interlayer tetrahedra. The formula of ganophyllite-group minerals can thus be written as $[Ca_x(K, Na)_y]^{[6]}(Mn_{6-z}Al_z)^{[4]}[Si_8(Al_{2x+y+z}Si_{2-2x-y-z})]\Sigma_{10}O_{24}(OH)_4{\cdot}nH_2O$. Because of the Al-Al avoidance rule arising from bonding considerations to the bridging O atoms of the interlayer tetrahedra, the interlayer tetrahedra can be no more than half-occupied by Al. The bond valence sums of the two tetrahedra (Si9, Si10, Table 4) support this suggestion, with bond valences of 3.50 and 3.51, respectively, suggesting Al:Si ~ 1:1 in those tetrahedra. Thus, $(2x + y + z) \leq 1$, in accord with the analyses of ganophyllite in Noe and Veblen (1999).

CHANNEL COMPONENTS

As in the Noe and Veblen (1999) study of ganophyllite, several distinct channel sites were located that were compatible with alkali/alkaline earth ions. Evaluation of the bond valence available to the channel cation sites showed that one site is compatible with ($Ca_{0.50}Na_{0.24}\square_{0.26}$) as obtained from EMPA and another is compatible with ($K_{0.34}\square_{0.66}$), also from the EMPA data. Although the effect of substantial vacancies on bond valence sums is not known, values of 0.88 valence units calculated using Na bond-valence constants and 1.39 valence units calculated using Ca constants (Brese and O'Keeffe 1991), are considered reasonable for the ($Ca_{0.50}Na_{0.24}\square_{0.26}$) site. Similarly, a bond-valence value of 0.85 valence units as calculated using K bond-valence constants for the ($K_{0.34}\square_{0.66}$) site is also reasonable. Several other sites of positive electron density were assigned as partially occupied water molecule sites, and

TABLE 8. Positions of all Mn and layer Si atoms in atomic arrangement of orthorhombic dimorph of tamaite, separated into triples of equivalent atoms in individual "subcells" of (3 × 5.6 Å) superstructure

				Mn Layers			
Mn2	0.0848	0.9974	0.0575	Mn2	0.0848	0.5026	0.0575
Mn6	0.4176	0.9977	0.0575	Mn6	0.4176	0.5023	0.0575
Mn3	0.7510	0.9855	0.0700	Mn3	0.7510	0.5145	0.0700
Mn4	0.2508	0.9901	0.1798	Mn4	0.2508	0.5099	0.1798
Mn5	0.5843	0.9820	0.1916	Mn5	0.5843	0.5180	0.1916
Mn1	0.9180	0.9822	0.1911	Mn1	0.9180	0.5178	0.1911
Mn5	0.0843	0.9820	0.3084	Mn5	0.0843	0.5180	0.3084
Mn1	0.4180	0.9822	0.3089	Mn1	0.4180	0.5178	0.3089
Mn4	0.7508	0.9901	0.3202	Mn4	0.7508	0.5099	0.3202
Mn3	0.2510	0.9855	0.4300	Mn3	0.2510	0.5145	0.4300
Mn2	0.5848	0.9974	0.4425	Mn2	0.5848	0.5026	0.4425
Mn6	0.9176	0.9977	0.4425	Mn6	0.9176	0.5023	0.4425
Mn6	0.0824	0.0023	0.5575	Mn6	0.0824	0.4977	0.5575
Mn2	0.4152	0.0026	0.5575	Mn2	0.4152	0.4974	0.5575
Mn3	0.7490	0.0145	0.5700	Mn3	0.7490	0.4855	0.5700
Mn4	0.2492	0.0099	0.6798	Mn4	0.2492	0.4901	0.6798
Mn1	0.5820	0.0178	0.6911	Mn1	0.5820	0.4822	0.6911
Mn5	0.9157	0.0180	0.6916	Mn5	0.9157	0.4820	0.6916
Mn1	0.0820	0.0178	0.8089	Mn1	0.0820	0.4822	0.8089
Mn5	0.4157	0.0180	0.8084	Mn5	0.4157	0.4820	0.8084
Mn4	0.7492	0.0099	0.8202	Mn4	0.7492	0.4901	0.8202
Mn3	0.2490	0.0145	0.9300	Mn3	0.2490	0.4855	0.9300
Mn6	0.5824	0.0023	0.9425	Mn6	0.5824	0.4977	0.9425
Mn2	0.9152	0.0026	0.9425	Mn2	0.9152	0.4974	0.9425

TABLE 8 – *continued*

				Si Layers			
Si5	0.3061	0.8952	0.0262	Si5	0.3061	0.6048	0.0262
Si1	0.6255	0.8823	0.0321	Si1	0.6255	0.6177	0.0321
Si6	0.9844	0.8867	0.0307	Si6	0.9844	0.6133	0.0307
Si2	0.1463	0.8814	0.1378	Si2	0.1463	0.6186	0.1378
Si3	0.4643	0.8774	0.1419	Si3	0.4643	0.6226	0.1419
Vacancy				**Vacancy**			
Si4	0.0254	0.4051	0.1960	Si4	0.0254	0.0949	0.1960
Si7	0.3652	0.4037	0.1944	Si7	0.3652	0.0963	0.1944
Si8	0.693	0.4069	0.2005	Si8	0.693	0.0931	0.2005
Si8	0.193	0.4069	0.2995	Si8	0.193	0.0931	0.2995
Si4	0.5254	0.4051	0.3040	Si4	0.5254	0.0949	0.3040
Si7	0.8652	0.4037	0.3056	Si7	0.8652	0.0963	0.3056
Si3	0.9643	0.6226	0.3581	Si3	0.9643	0.8774	0.3581
Si2	0.6463	0.6186	0.3622	Si2	0.6463	0.8814	0.3622
Si1	0.1255	0.6177	0.4679	Si1	0.1255	0.8823	0.4679
Si6	0.4844	0.6133	0.4693	Si6	0.4844	0.8867	0.4693
Si5	0.8061	0.6048	0.4738	Si5	0.8061	0.8952	0.4738
Vacancy				**Vacancy**			
Si5	0.1939	0.1048	0.5262	Si5	0.1939	0.3952	0.5262
Si6	0.5156	0.1133	0.5307	Si6	0.5156	0.3867	0.5307
Si1	0.8745	0.1177	0.5321	Si1	0.8745	0.3823	0.5321
Si2	0.3537	0.1186	0.6378	Si2	0.3537	0.3814	0.6378
Si3	0.0357	0.1226	0.6419	Si3	0.0357	0.3774	0.6419
Vacancy				**Vacancy**			
Si7	0.1348	0.5963	0.6944	Si7	0.1348	0.9037	0.6944
Si4	0.4746	0.5949	0.6960	Si4	0.4746	0.9051	0.6960
Si8	0.807	0.5931	0.7005	Si8	0.807	0.9069	0.7005
Si8	0.307	0.5931	0.7995	Si8	0.307	0.9069	0.7995
Si4	0.9746	0.5949	0.8040	Si4	0.9746	0.9051	0.8040
Si7	0.6348	0.5963	0.8056	Si7	0.6348	0.9037	0.8056
Si3	0.5357	0.3774	0.8581	Si3	0.5357	0.1226	0.8581
Si2	0.8537	0.3814	0.8622	Si2	0.8537	0.1186	0.8622
Vacancy				**Vacancy**			
Si1	0.3745	0.1177	0.9679	Si1	0.3745	0.3823	0.9679
Si6	0.0156	0.1133	0.9693	Si6	0.0156	0.3867	0.9693
Si5	0.6939	0.1048	0.9738	Si5	0.6939	0.3952	0.9738

Notes: Atoms in triples have approximate positions (*x, y, z*), [~(*x* + 1/3), ~*y*, ~*z*], and [~(*x* + 2/3), ~*y*, ~*z*].

others (<2.53 $e^{-}Å^{-3}$) could have been assigned. All channel sites were found to be partially occupied and some of the H_2O disordered.

The ability to place cations in large open channels, and also to control the number of available sites with $^{[4]}Al$ occupancy, makes the ganophyllite phases an intriguing host for large cations or organic molecules; we are currently investigating those properties in ion exchange experiments.

Supercell-subcell relationship in ganophyllite-group minerals

Previous studies of ganophyllite group phases have noted the presence of a "superstructure" along the ~5.6 Å axis. Such superstructures, evidenced through weak reflections that occur at 1/3 and 2/3 of the reciprocal lattice translations along **a*** (our setting), have been interpreted as indicating that the true cell of ganophyllite is merely an addition of three subcells along the ~5.6 Å axis, with minor perturbations of atomic positions and/or site occupancy in equivalent positions in the three subcells. In ganophyllite, it was suggested that the perturbations result from Al-Si ordering in the layer or interlayer tetrahedra (Noe and Veblen 1999).

If indeed ganophyllite-group minerals were true superstructures of the ~5.6 Å subcell described by Noe and Veblen, atomic positions along that axis (our **a** axis in *Pnma,* ~3 × 5.6 Å) would be such that each atom at (*x, y, z*) has equivalent atoms at [~(*x* + 1/3), ~*y*, ~*z*], and [~(*x* + 2/3), ~*y*, ~*z*], with the small deviations from these exact positions or their occupancies causing the weak superstructure reflections and the tripling of the unit cell. Table 8 lists the positions of all Mn atoms in the unit cell, and demonstrates that all Mn atoms do indeed exist in such sets of three. The Si atoms (Table 8) are similarly arranged, but with vacancies in 1/3 of the triples, which contribute to the superstructure. Finally, the interlayer tetrahedra also contribute to the superstructure reflections, as there are only two linkages along the (3 × 5.6 Å); therefore vacancies exist in the interlayer, as well. Thus, the (3 × 5.6 Å) subcell is not a true subcell, in that it does not have approximately equivalent atoms at (*x, y, z*), [~(*x* + 1/3), ~*y*, ~*z*], and [~(*x* + 2/3), ~*y*, ~*z*]. However, because of the nature of the atomic arrangement and vacancies in the layers that dominant the scattering, the $h = 3n$ reflections are much stronger than other diffractions. The large disparity between the very strong $h = 3n$ and the weak $h = (3n + 1)$ and $h = (3n + 2)$ reflections was evidenced in the inability of previous researchers to even measure the weak reflections with scintillation detectors. In addition, because the supercell-subcell relationship is not such that each atom has essential equivalents at (*x, y, z*), [~(*x* + 1/3), ~*y*, ~*z*], and [~(*x* + 2/3), ~*y*, ~*z*], earlier attempts at modeling the true structure of

ganophyllite as a supercell of the measured subcell led to incorrect predictions of the atomic arrangement. Although the majority of the scattering (e.g., all the Mn atoms and the majority of the Si atoms) exist in a supercell-subcell relationship, the lack of such a relationship for all atoms obviated a successful solution based on previous applications of the subcell-supercell relationship.

ACKNOWLEDGMENTS

The structure analysis portion of this work was supported by NSF grants EAR-9627222, Ear-9804768 (J.M.H.), and EAR-0003201 (J.M.H. and J.R.). Reviewers D. Peacor and J. Post are gratefully acknowledged for their perceptive comments. A. Pozzi of Genoa, Italy, is gratefully acknowledged for supplying the specimen.

REFERENCES CITED

Brese, N.E. and O'Keeffe, M. (1991) Bond-valence parameters for solids. Acta Crystallographica, B47, 192–197.

Brown, I.D. (1981) The Bond-Valence Method: An Empirical Approach to Chemical Structure and Bonding. In M. O'Keeffe and A. Navrotsky, Eds., Structure and Bonding in Crystals II, p. 1–30. Academic Press, New York.

Eggleton, R.A. and Guggenheim, S. (1986) A re-examination of the structure of ganophyllite. Mineralogical Magazine, 50, 307–315.

Guggenheim, S. and Eggleton, R.A. (1997) Modulated 2:1 Layer Silicates: Review, systematics, and predictions. American Mineralogist, 72, 724–738.

——— (1998) Crystal Chemistry, Classification and Identification of Modulated Layer Silicates. In S.W. Baily, Ed., Hydrous Phyllosilicates, 19, 675–725. Reviews in Mineralogy, Mineralogical Society of America, Washington, D.C.

Mandarino, J.A. (1981) The Gladstone-Dale relationship. IV. The compatibility concept and its application. Canadian Mineralogist, 19, 441–450.

Marchesini, M. and Pagano, R. (2001) The Val Graveglia Manganese District, Liguria, Italy. Mineralogical Record, 32, 349.

Marescotti, P. and Frezzotti, M.L. (2000) Alteration of braunite ores from Eastern Liguria (Italy) during syntectonic veining processes: mineralogy and fluid inclusions. European Journal of Mineralogy, 12, 341–356.

Matsubara, S., Imai, H., Miawaki, R., and Tokiko, T. (2000) Tamaite, the Ca-analogue of ganophyllite, from the Shiromaru Mine, Okutama, Tokyo, Japan. Journal of Mineralogical and Petrological Sciences, 95, 79–83.

Mottana, A., Ventura, G.D., Parodi, G.C., and Guidi, G. (1990) A calcium member of the ganophyllite group in the manganiferous metacherts of Molinello mine, Liguria, Italy. Atti della Accademia Nazionale dei Lincei. Rendiconti Lincei. Scienze Fisiche e Naturali Series 9, 1, 313.

Noe, D.C. and Veblen, D.R. (1999) Incommensurate modulation and the crystal structure of ganophyllite. American Mineralogist, 84, 1088–1098.

Peacor, D.R., Dunn, P.J., and Simmons, W.B. (1984) Eggletonite, the Na analogue of ganophyllite. Mineralogical Magazine, 48, 93–96.

Smith, M.L. and Frondel, C. (1968) The related layered minerals ganophyllite, bannisterite, and stilpnomelane. Mineralogical Magazine, 36, 893–913.

MANUSCRIPT RECEIVED AUGUST 27, 2002
MANUSCRIPT ACCEPTED FEBRUARY 3, 2003
MANUSCRIPT HANDLED BY KEVIN ROSSO